

## Fano interference and resonances in open systems

Arkady M. Satanin<sup>1,2</sup> and Yong S. Joe<sup>1</sup><sup>1</sup>Center for Computational Nanoscience, Department of Physics and Astronomy Ball State University, Muncie, Indiana 47306, USA<sup>2</sup>Institute for Physics of Microstructures, RAS, GSP-105 Nizhny Novgorod, 603950 Russia

(Received 27 September 2004; revised manuscript received 2 February 2005; published 27 May 2005)

A scenario of quantum interference in which decaying (quasibound) states interfere with the continuum or with other quasibound states is investigated. The model we adopt as the basis of our analysis consists of two or three antidots in an electronic waveguide. In a perfect waveguide, electron states belong to different subbands and antidots give a transfer between them. For a waveguide with two antidots we have observed interesting phenomena: interference between one subband of the quasibound state and a background second subband, and interference of resonant group states of different subbands. In this case, the zero of the Fano resonance is shifted to the complex plane and the coupling parameter becomes complex. In a waveguide with three antidots, degeneracy of two quasibound states takes place and interference of these states occurs. The Fano interference of two nearly degenerate resonances may bring a full suppression of pair resonances in the transmission. We explain that this is due to the parities of the quasibound states. Our results show that the zero of the Fano resonance due to interference between the quasibound states and the continuum is generally placed in the complex plane. This gives an additional possibility for manipulating conductance resonances in a waveguide by changing the antidot parameters.

DOI: 10.1103/PhysRevB.71.205417

PACS number(s): 73.23.Ad, 73.40.Gk, 73.63.Nm, 73.63.Kv

### I. INTRODUCTION

Tunneling and interference of electron waves in nanostructures are among the most important quantum phenomena.<sup>1,2</sup> Recently, Fano resonances have been extensively studied both theoretically and experimentally.<sup>3–20</sup> There are interesting manifestations of Fano resonances which have been observed in transport investigations of nanostructures.<sup>12,13,15,19,20</sup> Fano interference may potentially be used for the design of quantum electronic or spintronic devices, such as a Fano interference transistor<sup>15</sup> or a Fano filter for polarized electrons.<sup>21</sup> There is an attractive idea to use Fano phenomena for lasing without inversion.<sup>22</sup>

Many recent publications about Fano resonance in waveguides with an impurity (quantum dots with an attractive potential) have been reported.<sup>8–11,14,16–18</sup> In a theoretical investigation finding the positions and structure of resonances, the Feshbach formalism with a projection operator has been applied with success.<sup>23,24</sup> To explain the concept of excitations in interaction systems (as has been done for atomic systems), the shape of the conductance peaks can be understood in terms of single-electron configurations. In order to fit the experimental data, the authors used the expression for the conductance  $G$  of quantum waveguides, rings, and quantum islands:

$$G = G_b \frac{|\varepsilon + q|^2}{\varepsilon^2 + 1}, \quad (1)$$

where  $G_b$  is the nonresonant conductance, and  $\varepsilon = (E - E_R)/\Gamma$  is the reduced energy ( $E_R$  is the energy of the resonance,  $\Gamma$  is the width, and  $q$  is the coupling parameter).<sup>15,18</sup> Here, the parameter  $q$  measures qualitatively the interference between the bound states and propagating continuum states. Hence, the question is how to obtain the positions, widths, and  $q$  values of the long-living resonances. Fano resonance is

a phenomenon of the interference between the discrete levels and the continuum.<sup>3</sup> Since a discrete level has a real wave function, it is supposed in the original Fano theory that the coupling parameter is a real number.<sup>3</sup> Therefore, interference with a real wave function has been studied in most publications.<sup>3–11,14,16–18</sup>

When we consider resonance for a repulsive potential, the usual solutions of the Schrödinger equation for such a potential are real energy and continuum scattering states. The scattering functions form a complete set, and the continuum wave functions in principle describe all properties of the resonance. However, for energy near the resonance, the wave function looks like that of a bound state of the confinement potential. The resonance wave functions are linear combinations of such kinds of functions. For long-living resonances, the wave functions resemble more closely bound-state wave functions, and hence they form a more natural basis than the wave functions of the continuum states.<sup>24</sup> If the states that belong to the resonance are connected with the continuum, then we have an additional scenario of interference between decaying states and the continuum. This means that Fano resonances with a complex parameter  $q$  may be observed in the transmission.

Although the theory of Fano resonances has been developed in many publications, to the best of our knowledge, no attempt has been made to investigate the physical situations in which the parameter  $q$  is complex, or, in other words, when the zero of the Fano resonance is located in the complex energy plane. It is well known that Breit-Wigner (BW) resonance is an interference of waves in the same channel. Now an intriguing question arises: What happens when a group of resonance states interfere with other states of the continuum? The interference of a quasibound state with the continuum is similar to localized state interference, although it is not quite the same. The effect of Fano interference, which has been analyzed in detail in previous

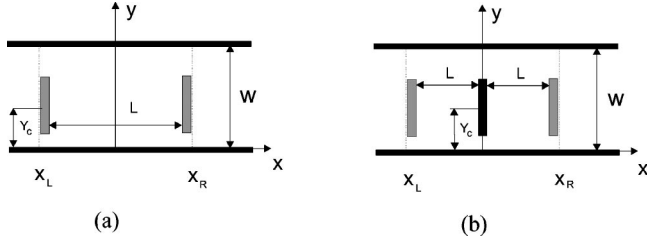


FIG. 1. An electron waveguide with (a) two and (b) three antidots. The inner potential domain ( $X_L < x < X_R$ ) is indicated by dotted lines at  $x = X_L$  and  $X_R$ . The width of antidots in the transverse direction is set to  $0.5W$  for all calculations.

articles,<sup>3–11,14–18</sup> emerges naturally as a result of the coupling between a discrete state from an attractive potential and the nearest bands of the continuum. While the interference between a single level and the continuum is the subject of many publications, interference between continuum states and another continuum has not been studied until very recently. The purpose of this paper is to investigate the interference of a narrow group of states with the continuum. We use a Feshbach method and analyze the evaluation of the scattering amplitude with repulsive potentials only when BW resonances are possible. In order to apply this method in this situation, it is necessary to assume the renormalization of the scattering parameters for direct processes. Therefore, we extend our discussion to the resonant theory of Kapura and Peierls,<sup>25</sup> which is more suitable to this purpose. A model we adopt as the basis of our analysis consists of two or three antidots in the waveguide, which may potentially be used for applications. It is implicitly assumed that electron-electron interactions play no further role in modifying the resonances, so that a single-particle approach is thus valid close to the resonance.<sup>26–28</sup>

## II. THE MODEL AND MAIN EQUATIONS

We study the propagation of the electron waves in an electronic two-dimensional (2D) waveguide of width  $W$  arranged along the  $x$  axis. Let us consider a confining potential  $V_c(y)$  in the transverse direction. Then, there is a complete basis of functions describing the transverse motion  $\varphi_n(y)$  of an electron with energies  $E_n$ , effective mass  $m$ , wave vector  $k_n$  along the  $x$  direction, and energy  $E = \hbar^2 k_n^2 / 2m + E_n$ . The electron waves in the perfect waveguide can be written as  $e^{\pm i k_n x} \varphi_n(y)$ . These propagating states may be considered in the waveguide as open channels. Now, we insert the repulsive potential  $V(x, y)$  of the antidots in the waveguide. The schematic geometry of the system is presented in Fig. 1 showing the potential region in the waveguide, where two or three antidots are arranged along the longitudinal direction and the potential outside of the region ( $X_L < x < X_R$ ) vanishes. Here, we introduce two or three antidots to demonstrate interference effects for both an isolated quasibound state (for two antidots) and degenerate quasibound states (for three antidots) with the continuum states.

In order to find an electron wave function in the waveguide with antidots, we solve the 2D Schrödinger equation

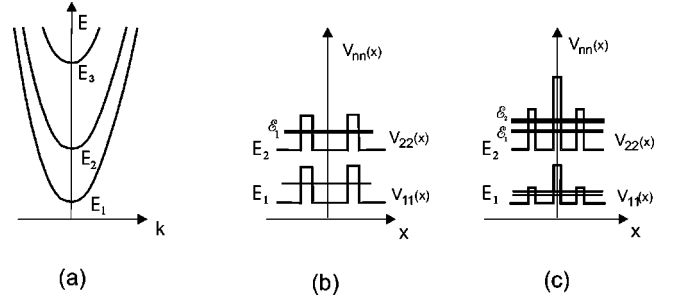


FIG. 2. (a) Dispersion relation for electron in a perfect waveguide, and (b) and (c) are schematic illustrations of the quasibound levels in the effective potentials for two and three antidots, respectively.

$$-\frac{\hbar^2}{2m} \left( \frac{\partial^2}{\partial x^2} + \frac{\partial^2}{\partial y^2} \right) \Psi(x, y) + V_c(y) \Psi(x, y) + V(x, y) \Psi(x, y) = E \Psi(x, y), \quad (2)$$

with particular boundary conditions in the leads ( $x \rightarrow \pm\infty$ ). It is convenient to expand the wave function in the complete basis of functions describing the transverse motion:

$$\Psi(x, y) = \sum_{n=1}^{\infty} \psi_n(x) \varphi_n(y). \quad (3)$$

Substituting expansion Eq. (3) into Eq. (2), we obtain the coupled-channel equations for an electron in the form

$$-\frac{\hbar^2}{2m} \frac{\partial^2}{\partial x^2} \psi_n(x) + \sum_{n'=1}^{\infty} V_{nn'}(x) \psi_{n'}(x) = (E - E_n) \psi_n(x), \quad (4)$$

where the coupling matrix elements of the antidot's potential (which still act on the  $x$  coordinate) are defined to be

$$V_{n,n'}(x) = \int \varphi_n(y) V(x, y) \varphi_{n'}(y) dy. \quad (5)$$

Since Eq. (4), which is equivalent to the 2D Schrödinger equation, cannot be solved in general, we use some parameters which allow us to use a resonant perturbation theory<sup>23,24</sup> in the system under investigation. Here, we consider the situation when the energy of the incoming electron is placed in the interval  $E_2 \langle E_3$  (the second energy window), as shown schematically in Fig. 2.

It was shown in Refs. 29 and 30 that the calculation of the conductance in a waveguide with quantum dots in the ballistic regime reduces to the solution of the scattering problem. We are interested in the transmission amplitude  $t_{n,n'}$  describing the scattering of electrons from the channel with number  $n'$  into the channel with number  $n$ . The transmission amplitude can be determined from the asymptotic solutions of Eq. (4). The conductance measured by the two-probe method is determined by the Buttiker-Landauer formula<sup>1,29,30</sup> through a scattering matrix.

### III. FANO INTERFERENCE OF RESONANCES WITH THE CONTINUUM

In this section, we try to understand how the group of resonances interacts with the continuum. Investigation of a waveguide with an attractive impurity has shown that having more than two open channels only alters the width and position of the resonances, and hence plays a minor role in the Fano phenomenon.<sup>8-10</sup> Therefore, in the resonant approximation we only need to consider two coupled equations in the second energy window ( $E_2 \langle E_3$ ) to understand the main physical features of the interference. If the characteristic value of the matrix element  $V_{12}$ , describing the coupling between two nearest channels, is small compared to the subband distance, then we can use the two-band approximation in the form

$$\left(-\frac{\hbar^2}{2m} \frac{\partial^2}{\partial x^2} + V_{11}(x)\right) \psi_1(x) + V_{12}(x) \psi_2(x) = (E - E_1) \psi_1(x), \quad (6)$$

$$\left(-\frac{\hbar^2}{2m} \frac{\partial^2}{\partial x^2} + V_{22}(x)\right) \psi_2(x) + V_{21}(x) \psi_1(x) = (E - E_2) \psi_2(x). \quad (7)$$

However, without much problem this can be extended for a multiband approximation.

In order to examine the interaction between the group of resonances and the continuum, we use two different methods which can both illuminate the coherent effects in the transmission. First, we extract a resonant contribution from the scattering amplitude. In other words, we try to find a dispersion formula for the transmission in an open system. Second, we solve Eqs. (6) and (7) by using a numerical method and obtain the transmission amplitude. In this case, we evaluate the conductance numerically in the quantum channel with two and three antidots. The advantage of this technique is that tuning of the resonance is possible by modulating the parameters of the system. In addition, the overlapping of resonances is also shown in the waveguide with three antidots. In our numerical calculations performed here, we use the following parameters for the waveguide and antidots: the effective mass  $m=0.067m_0$  (which is appropriate for the AlGaAs/GaAs interface) and the width of the waveguide is  $W=23.69$  nm (which gives  $E_1=10$  meV and  $E_2=40$  meV for the first two energy levels due to transverse confinement in the waveguide). The distance  $L$  between antidots, and the position  $Y_c$  of the middle of the antidots in the waveguide are also parameters of the system, as shown in Fig. 1; these parameters may be considered as variables.

#### A. Decoupled systems

First, we study an analysis of the decoupled systems [ $V_{12}(x)=0$ ]. If we neglect intersubband interactions, the incoming decoupled wave in the first channel may be found from

$$\left(-\frac{\hbar^2}{2m} \frac{\partial^2}{\partial x^2} + V_{11}(x)\right) \chi_E^\pm(x) = (E - E_1) \chi_E^\pm(x). \quad (8)$$

Here,  $\chi_E^+(x)$  and  $\chi_E^-(x)$ , which are solutions of Eq. (8), have the asymptotic form

$$\chi_E^\pm(x) = \begin{cases} \tau_1^\pm e^{\pm ik_1 x}, & x \rightarrow \pm \infty, \\ e^{\pm ik_1 x} + \rho_1^\pm e^{\mp ik_1 x}, & x \rightarrow \mp \infty, \end{cases} \quad (9)$$

where  $\tau_1^\pm$  and  $\rho_1^\pm$  are the transmission and reflection amplitudes ( $\tau_1^+ = \tau_1^- \equiv \tau_1$ ).<sup>1</sup> In other words, we assume that in the first channel there are only nonresonant states for a given energy interval.

In decoupled systems, the wave functions in the second channel belong to the continuum. In order to treat the scattering problem for a repulsive potential, which produces quasibound states, the resonant states are more convenient to use because the resonant wave functions form a more natural basis than the functions of the continuum. We use Kapura's and Peierls' (KP) approach<sup>25</sup> which gives orthogonal functions of the quasibound states. In order to find the KP basis, we solve the auxiliary equation in the potential region ( $X_L < x < X_R$ )

$$\left(-\frac{\hbar^2}{2m} \frac{\partial^2}{\partial x^2} + V_{22}(x)\right) \phi_j(x) = (\varepsilon_j - E_2) \phi_j(x), \quad (10)$$

with special boundary conditions (the radiation or Sommerfeld boundary conditions) (see Appendix A for details). The solutions of Eq. (10) produce resonant states with complex energies and eigenfunctions:

$$\varepsilon_j = \varepsilon_j^R - i\gamma_j^R, \quad \phi_j(x) (j=1, 2, \dots). \quad (11)$$

If the distance between resonances is greater than the width and the energy of the incoming electron is located near the energy of a resonance, then we can consider a contribution of each resonant state separately. In this case, we have a resonance in the second channel with a Lorentzian line shape. There are situations when a group of overlapping resonances may be in the second channel. In this case the shape of the resonances in the overlapping group will be different from Lorentzian (see Sec. III D for details).

Thus, for the decoupled system we have scattering waves  $\chi_E^+(x)$  and  $\chi_E^-(x)$  in the first channel, and quasibound states  $\phi_j(x)$  in the second channel. For the coupled channel, on the other hand, the interaction may induce a transition from propagating states to quasibound states. In other words, the interaction may induce interference between the quasibound states and the continuum.

#### B. Interference of resonances with background

We are interested in the case in which the energy of an incoming electron is assumed to be located near the resonant energy, defined by Eq. (11). For the coupled systems, the wave function  $\psi_2(x)$  may be expanded in the interval  $X_L < x < X_R$  as

$$\psi_2(x) = \sum A_j \phi_j(x). \quad (12)$$

From Eq. (7) we can find a formal expression for the amplitudes  $A_j$ ,

$$(E - \varepsilon_j)A_j = (\phi_j | V_{12} | \psi_1), \quad (13)$$

where the scalar product in right side of Eq. (13) defined in Appendix A. Using a Green's function for the electron in the first decoupled channel, the solution of Eq. (6) can be written as

$$|\psi_1\rangle = |\chi_E^+\rangle + G_1^+ V_{12} |\psi_2\rangle, \quad (14)$$

where  $|\chi_E^+\rangle$  is the amplitude of the incoming wave in the first decoupled channel. Substituting Eq. (14) into Eq. (13), we obtain the following explicit equation for the amplitudes:

$$(E - \varepsilon_j)A_j - \sum_{j'} U_{jj'} A_{j'} = (\phi_j | V_{21} | \chi_E^+), \quad (15)$$

where

$$U_{jj'} = (\phi_j | V_{21} G_1 V_{12} | \phi_{j'}). \quad (16)$$

If we assume that the incoming wave belongs to the first channel, we can find the elements of the scattering matrix that are determined by the asymptotic behavior of the outgoing wave  $\psi_1(x)$ : for  $x \rightarrow +\infty$ ,  $\psi_1(x) \rightarrow t_{11} e^{ik_1 x}$ . To do this, we use Eq. (14) in the form

$$\psi_1(x) = \tau_1 e^{ik_1 x} + \sum_j A_j \int dx' G_1^+(x, x') V_{12}(x') \phi_j(x'), \quad (17)$$

where the explicit form of the Green's function is

$$G_1^+(x, x') = \frac{m}{ik_1 \hbar^2 \tau_1} \times \begin{cases} \chi_E^+(x) \chi_E^-(x'), & x > x', \\ \chi_E^-(x') \chi_E^+(x), & x < x', \end{cases} \quad (18)$$

where  $\chi_E^+(x)$  and  $\chi_E^-(x)$  are solutions of Eq. (8) and  $\tau_1$  is the scattering amplitude in the first channel. We use expressions that connect the asymptotic behavior of  $\chi_E^+(x)$  and  $\chi_E^-(x)$  with the reflection and transmission coefficients.<sup>9,10</sup> Substituting the solution of Eq. (15) into Eq. (17), we obtain the explicit equation for the amplitude  $t_{11}$  in the form

$$t_{11} = \tau_1 \left\{ 1 + \frac{m}{ik_1 \hbar^2 \tau_1} \sum_{jj'} (\chi_E^- | V_{12} | \phi_j) \left( \frac{I}{E - H} \right)_{jj'} (\phi_{j'} | V_{12} | \chi_E^+) \right\}, \quad (19)$$

where  $H = \varepsilon I + U$  is defined as a matrix, and  $I$  is a unit matrix.

Similarly, considering the wave function  $\psi_2(x)$  to have asymptotic behavior  $\psi_2(x) \rightarrow t_{21} e^{ik_2 x}$ , for  $x \rightarrow \infty$ , we obtain

$$t_{21} = e^{-ik_2 x_R} \sum_{jj'} \phi_j(x_R) \left( \frac{I}{E - H} \right)_{jj'} (\phi_{j'} | V_{12} | \chi_E^+). \quad (20)$$

Similar expressions for  $t_{12}$  and  $t_{22}$  can also be found. These expressions can be simplified for a particular energy interval by taking into account only a finite number channels which interfere with the continuum resonant states. Equations (19) and (20), called dispersion formulas for the transmission am-

plitudes, are the main results of this section. To illustrate the result for the transmission amplitudes, we consider the simple case when only a single resonance is in the first energy window of the second channel.

### C. Separate resonances

Let us consider the appropriate parameters of antidots for a single resonance in the second channel. It is assumed that the distance between resonances is greater than the width of the resonance for a given energy interval [see Fig. 2(b)]. In this case, we examine a single quasibound state in the potential  $V_{22}(x)$  and choose the state with the number  $j=1$ . From Eq. (19) we obtain

$$t_{11} = \tau_1 \frac{E - \tilde{E}_1^0}{E - E_1^R + i\Gamma_1^R}, \quad (21)$$

where  $E_1^R = \varepsilon_1^R + \text{Re}(U_{11})$  and  $\Gamma_1^R = \gamma_1^R - \text{Im}(U_{11})$ . Here, the complex pole and zero are obtained by  $\tilde{E}_1^R = \varepsilon_1 + U_{11}$  and  $\tilde{E}_1^0 = \varepsilon_1 + Q_{11}$ , respectively. The complex parameter  $Q_{11}$  is defined as the matrix element

$$Q_{jj'} = \frac{m}{ik_1 \hbar^2 \tau_1} \left( \int_{-X_L}^{X_R} dx \phi_j(x) V_{12}(x) \int_x^{X_R} dx' \phi_{j'}(x') V_{12}(x') \right. \\ \left. \times [\chi_E^+(x') \chi_E^-(x) - \chi_E^-(x') \chi_E^+(x)] \right). \quad (22)$$

Notice that all parameters of the resonance (zero and pole) are slowly varying functions of energy.

Thus, we obtain a simple result for the transmission amplitude with a zero and a pole in the complex energy plane. However, the meaning of this result is different from the interference of a *bound state* with the continuum. Two contributions to the width of the resonance are as follows: (a) the width of the quasibound level  $\gamma_1^R$  and (b)  $\text{Im}(U_{11})$ , which is the result of interference with the resonance with the continuum. The equation  $\tilde{E}_1^0 = \varepsilon_1 + Q_{11}$  implies that the zero of the resonance is generally located in the complex plane. Since  $\gamma_1^R - \text{Im} Q_{11}$  is equal to zero for the bound-state energy (see proof in Refs. 10 and 17), the transmission amplitude has a zero on the real energy axis. In this case, the position of zero resonance is defined by  $E_1^0 = \varepsilon_1^R + \text{Re}(Q_{11})$ . Then, Eq. (21) gives the contribution of the Fano line shape, shown in Eq. (1), to the conductance due to the current in the first channel with the complex parameter

$$q = \{\text{Re}(U_{11} - Q_{11}) + i[\gamma_1^R - \text{Im}(Q_{11})]\} / [\gamma_1^R - \text{Im}(U_{11})].$$

In addition, there is another contribution to the conductance from the second channel when the Fermi energy belongs to the second energy window. Near the resonant energy, the transmission amplitude  $t_{21}$  can be obtained from Eq. (2) as

$$t_{21} \approx e^{-ik_2 x_R} \frac{(\chi_E^- | V_{12} | \phi_1) \phi_1(x_R)}{E - E_1^R + i\Gamma_1^R}. \quad (23)$$

The obtained results for  $t_{11}$  and  $t_{21}$  have a simple physical interpretation as follows. The antidots in the waveguide form

an open resonator. Assuming that an incoming wave is in the first channel ( $n=1$ ) and interacts with the antidots, the wave may be transferred to an open resonator in the second channel ( $n=2$ ). In this case, we have slowly emitted waves in the second channel. So, if there is a resonant state in the second channel (i.e., there are only outgoing waves), it gives a Lorentz-type resonance in the transmission. In the meantime, the interference between a nonresonant state (background) in the first channel and a quasibound state in the second channel gives a Fano-type profile in the transmission. The same results are expected when a nonresonant state in the second channel interferes with a resonant state in the first channel.

For a numerical calculation we assume that the antidots are described by short-range potentials in the direction of electron propagation, and finite in the transverse direction. The matrix elements of the antidot potentials may be written in the form

$$V_{n,n'}(x) = \frac{\hbar^2}{m} v_{n,n'} \left[ \delta\left(x - \frac{L}{2}\right) + \delta\left(x + \frac{L}{2}\right) \right], \quad (24)$$

where  $v_{n,n'}$  is the matrix of the single-dot potential defined by the width of the waveguide  $W$ , the position of the barriers  $Y_c$  (defined from the edge of the waveguide to the center of the barrier), and the scattering parameters  $aV_0$  ( $V_0$  is the potential barrier height, and  $a$  is the thickness of the barrier). The transverse geometrical parameter (the width of the scatterers) is set to  $0.5W$  for all the antidots. The matrix element  $v_{n,n'}$  for a system under consideration [see Figs. 1(a) and 1(b)] can be easily obtained from Eq. (5) in an explicit form. Then, Eqs. (6) and (7) for a given potential in the two-band approximation may be solved by using transfer-matrix techniques [1].

We have calculated the transmissions

$$T_{1 \rightarrow 1,2} = |t_{11}|^2 + \frac{k_2}{k_1} |t_{21}|^2 \quad \text{and} \quad T_{2 \rightarrow 2,1} = |t_{22}|^2 + \frac{k_1}{k_2} |t_{12}|^2 \quad (25)$$

for different positions of the antidots by varying the parameter  $Y_c$ . This parameter characterizes the transfer of the waves between two channels. If  $Y_c = 0.5W$ , the antidots are placed in the center of the waveguide and the interaction between channels is equal to zero (decoupled channels). For a given distance between antidots ( $L=27$  nm) there are BW resonances in the second channel in the second energy window ( $E_2 \langle E \langle E_3$ ). In order to obtain the energy value of the resonance, we solve the KP equation for the potential given in Eq. (24). The energy can then be found from

$$\sin\left(\frac{q_n L}{2}\right) = \frac{1}{2i} \left[ \left( \frac{\kappa_n + iq_n}{\kappa_n - iq_n} \right)^2 - 1 \right] e^{-iq_n L/2}, \quad (26)$$

where  $q_n = \sqrt{2m(\varepsilon - E_n)}/\hbar$  and  $\kappa_n = ik_n - 2v_{nn}$  ( $n=1,2$ ). Suppose we focus on the resonance with the position  $\varepsilon_1^R = 46.33$  meV and the width  $\gamma_1^R = 0.18$  meV (for noninteracting channels,  $Y_c = 0.5W$ ). In general, the interaction between channels changes the shape of the resonance dramatically. The transmission in the first and second channels as a function of the electron energy is shown in Fig. 3 for different

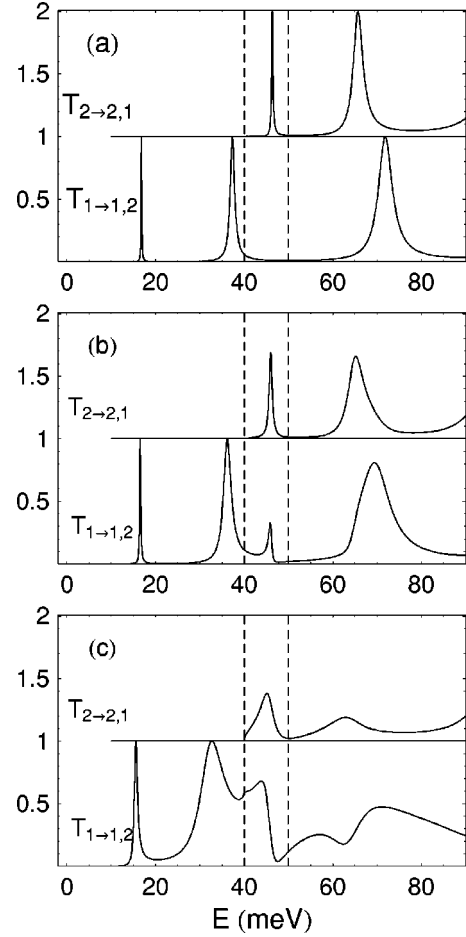


FIG. 3. Transmissions  $T_{1 \rightarrow 1,2}$  and  $T_{2 \rightarrow 2,1}$  of a quantum waveguide with two antidots as a function of the electron energy for three different positions of the antidots:  $Y_c =$  (a)  $0.5W$ , (b)  $0.375W$ , and (c)  $0.25W$ . The vertical dashed lines parcel out the energy interval where an effective Fano interference takes place for the given parameters of system (from 40 to 50 meV). The distance between the antidots is  $L=27$  nm, and the scattering parameter is  $aV_0 = 0.8$  eV nm, where  $a$  is the length of the antidot and  $V_0$  is the height of the potential barrier. The pronounced BW resonances in the first and second channels are shown in (a). We focus on the first resonance in the second channel with the position  $\varepsilon_1^R = 46.33$  meV and the width  $\gamma_1^R = 0.18$  meV.

values of the coupling parameter (the position  $Y_c$  of antidots). As the energy of the propagating electron is changed, the effective matrix element of channel interaction is changed from destructive to constructive interference. For an attractive potential, the wave function of the discrete levels is real and the zero of the resonance is on the real axis of the energy. Hence, the transmission goes through zero when the electron energy goes through the particular energy of Fano resonance. The interaction of resonances in an open system results in the shift of the zero resonance in the complex energy plane, and the transformation of a BW resonance into a Fano resonance in the first channel. The transmission  $T_{11} = |t_{11}|^2$  of the first channel, indicating the Fano resonance, is shown in Fig. 4(a) and the transmission  $T_{22} = |t_{22}|^2$  of the second channel, indicating a transformation of BW resonance, is depicted in Fig. 4(b) for  $Y_c = 0.425W$  when there is

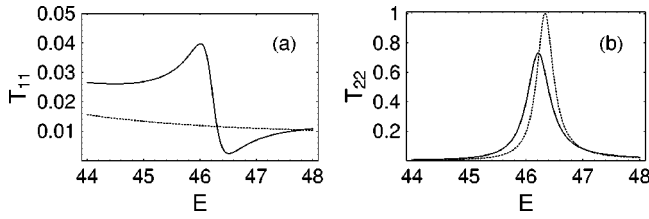


FIG. 4. Transmission (a)  $T_{11}$  of the first channel and (b)  $T_{22}$  of the second channel for a waveguide with two antidots as a function of the electron energy for  $Y_c=0.425W$  (solid line) and  $0.5W$  (dotted line). A Fano resonance is seen in  $T_{11}$ , whereas a transformation of the BW resonance is in  $T_{22}$  due to the interference between channels. Other parameters are the same as in Fig. 3.

interference between channels. In order to see the shift of the zero resonance in the complex energy plane, we present a contour plot of the absolute value of the transmission amplitude for the Fano and BW resonances in Figs. 5(a) and 5(b), respectively. In Fig. 5(a), we see a Fano dipole (transmission zero and pole) in the complex energy plane where the energies of a zero and a pole are  $\tilde{E}_1^0=(46.47-i0.14)$  meV and  $\tilde{E}_1^R=(46.21-i0.24)$  meV, respectively. This clearly indicates that the position of the transmission zero is shifted to the complex energy plane due to the interference between channels. We note that the position of a pole in the second channel is approximately the same as that of the first channel for  $Y_c=0.425W$ , but it is shifted a little for the nonperturbed resonance ( $Y_c=0.5W$ ) as  $\tilde{E}_1^R=(46.33-i0.18)$  meV.

The conductance of the waveguide with two antidots as a function of the electron energy is shown in Fig. 6(a), and the shape of the Fano resonance [marked by an arrow in Fig. 6(a)] on a different scale is depicted in Fig. 6(b). The shape of the Fano resonance in the conductance of the waveguide for different positions of the antidots is displayed in Fig. 7. Thus, if a long-living state interferes with the continuum, the zero of Fano resonance is placed in the complex plane.

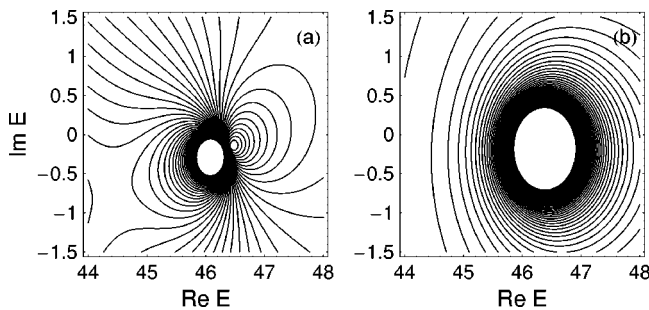


FIG. 5. A contour plot of the absolute value of the transmission amplitudes ( $T_{11}$  and  $T_{22}$ ) in the complex energy plane is depicted for (a) Fano and (b) BW resonances for the same parameters as in Fig. 4. (a) The position of the transmission zero is shifted to the complex energy plane due to the interaction of resonance with continuum [ $\tilde{E}_1^0=(46.47-i0.14)$  meV] and (b) a transformation from Fano resonance to BW resonance in the first channel is observed with evidence of merging a Fano dipole (transmission zero and pole) and a transmission pole.

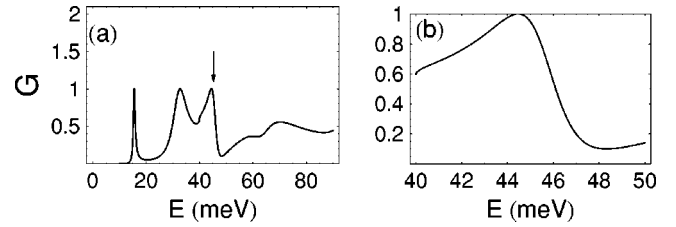


FIG. 6. (a) Conductance of the waveguide with two antidots for  $Y_c=0.3W$  (in units of the nonresonant conductance of the waveguide). The Fano resonance is a result of interference between the second channel of the quasibound states and the first channel of the continuum (Fano resonance is marked by an arrow). (b) The shape of the Fano resonance in the conductance is depicted in a different scale. Other parameters are the same as in Fig. 4.

#### D. Overlapping of resonances and Fano interference

To begin this subsection, we discuss the interference of the localized states. For instance, when two identical quantum wells are brought together to a distance comparable with their localized radius, the degenerate levels become split due to the interference of the waves. A similar effect takes place for quasibound states. When more than one resonant quasibound state is present in a one-channel system, for instance, in a three-barrier system,<sup>33,34</sup> the resonance states interfere with each other and this results in the overlapping of resonances. Since the interaction between resonance states gives the overlapping of resonances, the single BW formula is no longer valid for this situation.

In the triple-barrier resonant structure of Fig. 2(c), in particular, there are two resonant quasibound states which are associated with bonding and antibonding states in the two wells separated by a barrier. In order to consider tunneling through this system of three antidots, we add an additional antidot at the origin with matrix elements  $v_{n,n}^c$  to Eq. (5). Then, the new matrix elements of the three-antidot potentials can be written as

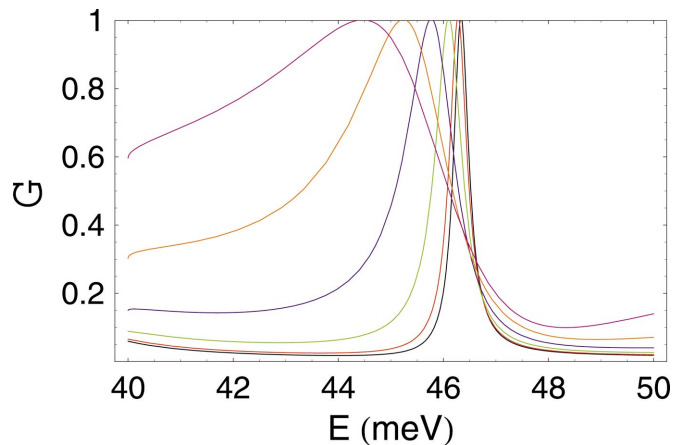


FIG. 7. (Color) Fano resonance in the conductance of the waveguide for different positions of the antidots:  $Y_c=0.5W$  (black),  $0.45W$  (red),  $0.4W$  (green),  $0.35W$  (blue),  $0.3W$  (brown), and  $0.25W$  (purple). Other parameters are the same as in Fig. 4.

$$V_{n,n'}(x) = \frac{\hbar^2}{m} \left\{ \nu_{n,n'}^c \delta(x) + \nu_{n,n'} \left[ \delta\left(x - \frac{L}{2}\right) + \delta\left(x + \frac{L}{2}\right) \right] \right\}. \quad (27)$$

Now, we have the possibility of manipulating resonances by changing the potential height of this additional antidot at the origin.

In this section, we extend these studies to consider the interference of two quasibound states with a continuum. Here, we focus on the case where the two quasibound states are in the second channel (for a decoupled system). It is clear that two quasibound states can interact only through virtual transitions to the continuum, because the interaction of the resonance with the continuum is defined by Eq. (15). It can be seen that for a system with symmetry about the center the “initial” quasibound levels do not interact directly ( $U_{12}=0$ ), but are connected through the matrix element describing the transition from the quasibound levels to the first band. We can find from Eq. (19) that the transmission amplitude for this case has the form

$$t_{11}(E) = \tau_1(E) \frac{(E - \tilde{E}_1^0)(E - \tilde{E}_2^0) + \gamma_{12}^2}{(E - E_1^R + i\Gamma_1^R)(E - E_2^R + i\Gamma_2^R)}, \quad (28)$$

where

$$\gamma_{12}^2 = \frac{m^2}{\hbar^4 k_1^2 \tau_1^2} (\chi_E^- |V_{21}| \phi_1) (\chi_E^- |V_{21}| \phi_2) (\phi_1 |V_{21}| \chi_E^+) (\phi_2 |V_{21}| \chi_E^+),$$

$E_j^R = \varepsilon_j^R + \text{Re}(U_{jj})$ ,  $\Gamma_j^R = \gamma_j^R - \text{Im}(U_{jj})$ , and  $\tilde{E}_j^0 = \varepsilon_j + Q_{jj}$  ( $j=1,2$ ). Here, the complex parameters  $Q_{jj}$  are defined by Eq. (22) and the coupling parameter  $\gamma_{12}$  can be obtained from the framework of the matrix potential Eq. (27) in an explicit form. As a result of the interference, the positions of the zeros in the complex energy plane depend on the coupling parameters between the localized states and the continuum. The scattering amplitude also possesses two poles in the complex plane. Thus, Fano resonances interact effectively and this leads to a number of interesting consequences, as will be proved below.

We present numerical results to illuminate the interference of two quasibound states with a continuum. The levels in the system with three antidots may be found by perturbation theory. For instance, if the distance between the antidots is  $L=27$  nm for given barriers, there are two quasibound states for energies  $\varepsilon_1^R=43.56$  meV ( $\gamma_1^R=0.37$  meV) and  $\varepsilon_2^R=45.64$  meV ( $\gamma_2^R=0.80$  meV), which give two overlapping resonances in the transmission. The transmissions  $T_{1 \rightarrow 1,2}$  and  $T_{2 \rightarrow 2,1}$  as a function of energy for different positions of three antidots [ $Y_c=(a) 0.5W$ , (b)  $0.4W$ , and (c)  $0.3W$ ] are shown in Fig. 8. It can be clearly seen that there are two overlapping BW resonances in the second channel. The asymmetric Fano resonance in the transmission is due to the interference of resonances with the continuum.

#### IV. INTERFERENCE OF RESONANCES IN DIFFERENT CHANNELS

Now, a very interesting question arises: what happens when both scattering channels have resonances with nearby

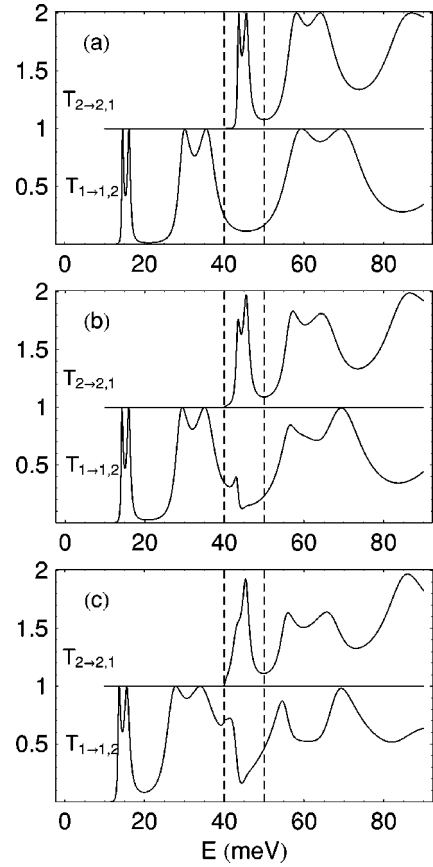


FIG. 8. Transmissions  $T_{1 \rightarrow 1,2}$  and  $T_{2 \rightarrow 2,1}$  for different positions of the three antidots:  $Y_c=(a) 0.5W$ , (b)  $0.4W$ , and (c)  $0.3W$ . The distance between the antidots is  $L=27$  nm, and the amplitude of the intermediate antidot potential is chosen to be 1.25 larger than the others; the scattering parameter is  $aV_0=0.4$  eV nm. There is an overlapping of the BW resonances in the second channel which gives an asymmetric (Fano-type) resonance in the transmission.

positions? Since crossing of the resonances is possible in this case (see below), we need to modify the method for investigating the interference of resonances in open systems. We begin by studying the analysis of the KP equations for coupled channels:

$$\begin{aligned} \left( -\frac{\hbar^2}{2m} \frac{\partial^2}{\partial x^2} + V_{11}(x) \right) \phi_{1j}(x) + V_{12}(x) \phi_{2j}(x) &= (\varepsilon_j - E_1) \phi_{1j}(x), \\ \left( -\frac{\hbar^2}{2m} \frac{\partial^2}{\partial x^2} + V_{22}(x) \right) \phi_{2j}(x) + V_{21}(x) \phi_{1j}(x) &= (\varepsilon_j - E_2) \phi_{2j}(x). \end{aligned} \quad (29)$$

From now on, we use the notation  $\varepsilon_j = E_j^R - i\Gamma_j^R$  throughout the section. The wave functions in the inner potential region may be expanded as

$$\psi_1(x) = \sum A_j \phi_{1j}(x), \quad \psi_2(x) = \sum A_j \phi_{2j}(x). \quad (30)$$

Using Eq. (29) and boundary conditions (see Appendix B), we can finally find the elements ( $t_{11}$  and  $t_{21}$ ) of the transmission amplitude:

$$\begin{aligned}
t_{11} &= \frac{i\hbar^2 k_1 e^{-ik_2 X_R}}{m} \sum_j \frac{\phi_{1j}(X_R) \phi_{1j}(X_L)}{E - E_j^R + i\Gamma_j^R}, \\
t_{21} &= \frac{i\hbar^2 k_1 e^{-ik_2 X_R}}{m} \sum_j \frac{\phi_{1j}(X_R) \phi_{2j}(X_L)}{E - E_j^R + i\Gamma_j^R}.
\end{aligned} \tag{31}$$

Similarly, the elements ( $t_{22}$  and  $t_{12}$ ) of the scattering matrix can also be obtained if the incoming wave is only in the second channel.

### A. Interference of two resonances in continuum

We start our analysis considering a two-antidot system with no coupling between channels. In this case, we have two independent KP equations from Eq. (29) with  $V_{12}=0$ . If we also assume that the antidot barriers are very high, then we can find the solutions of independent KP equations using a perturbation. In the first approximation, we have energies for the first and the second channels

$$\varepsilon_{1,j}^{(0)} = E_1 + \frac{\pi^2 \hbar^2 j^2}{2mL^2} \quad \text{and} \quad \varepsilon_{2,s}^{(0)} = E_2 + \frac{\pi^2 \hbar^2 s^2}{2mL^2}, \tag{32}$$

with  $j, s=1, 2, \dots$ , respectively. It is easy to show that there are solutions of the equations

$$\varepsilon_{1,j}^{(0)}(L) = \varepsilon_{2,s}^{(0)}(L) \tag{33}$$

if we treat the distance  $L$  as a free parameter in this equation. In other words, by changing the distance between antidots, we get two closely placed quasilevels. If the distance between quasilevels is less than the width of the resonances, the corresponding states may be considered as almost degenerate. The weak coupling between the channels by a matrix element  $V_{12}$  gives the interference between the quasibound states.

Let us use the condition of resonant overlapping that takes place for a particular distance between the antidots. For the unperturbed system, we have two solutions of the decoupled equations (29):

$$\phi_1(x) \equiv \phi_{1,j}(x), \quad \varepsilon_1 \equiv \varepsilon_{1,j},$$

and

$$\phi_2(x) \equiv \phi_{2,s}(x), \quad \varepsilon_2 \equiv \varepsilon_{2,s}. \tag{34}$$

For a weak coupling interaction between channels, the solution of Eq. (29) can be written in the form

$$\begin{pmatrix} \Phi_1(x) \\ \Phi_2(x) \end{pmatrix} = c_1 \begin{pmatrix} \phi_1(x) \\ 0 \end{pmatrix} + c_2 \begin{pmatrix} 0 \\ \phi_2(x) \end{pmatrix}. \tag{35}$$

From Eqs. (29), we also can find the perturbed energies of the resonances  $\varepsilon_{\pm}$ :

$$\varepsilon_{\pm} = \frac{\varepsilon_1 + \varepsilon_2}{2} \pm \sqrt{\left(\frac{\varepsilon_1 - \varepsilon_2}{2}\right)^2 + (1|V_{12}|2)^2}, \tag{36}$$

where the element of the complex matrix is defined by

$$(1|V_{12}|2) = \int_{X_L}^{X_R} \phi_1(x) V_{12}(x) \phi_2(x) dx. \tag{37}$$

Note that Eq. (36) is written using complex parameters ( $\varepsilon_{\pm} = E_{\pm}^R - i\Gamma_{\pm}^R$ ), even though it looks like the usual expression for splitting and degenerate energy levels in perturbation theory. This equation describes the interaction of poles in the complex energy plane. Thus, the solutions of Eq. (36) give the position and the width of the resonances. Applying a standard method, we can find two orthogonal wave functions  $\Phi_{\pm}$  for the complex eigenvalues  $\varepsilon_{\pm}$ . Using these functions, we can expand the transmission amplitude near the resonances as is done in Eq. (31). Therefore, in the first scattering channel we have

$$t_{11} \approx \frac{i\hbar^2 k_1 e^{-ik_2 X_R}}{m} \left( \frac{\Phi_+(X_R)\Phi_+(X_L)}{E - E_+^R + i\Gamma_+^R} + \frac{\Phi_-(X_R)\Phi_-(X_L)}{E - E_-^R + i\Gamma_-^R} \right). \tag{38}$$

Each term in Eq. (38) describes a resonance with a Lorentzian line shape. Because the wave functions are complex, phase interference of resonances in the transmission is possible. An example of this type of interference is presented in Fig. 9 for different positions of the antidots, with the distance between the antidots  $L=36.46$  nm. There is a dip in the first channel of the transmission due to the interference of two resonances between the first and second channels. The dip is located near the bare energy  $\varepsilon_{1,3}^{(0)} = \varepsilon_{2,1}^{(0)} = 43.36$  meV ( $\gamma_{1,3}^R = 1.34$  meV,  $\gamma_{2,1}^R = 0.13$  meV). The resonance in the second channel shows an asymmetric shape in Fig. 9(c). The conductance of the waveguide, which is the sum of the transmission of the different channels, as a function of Fermi energy in the regime of overlapping resonance is shown in Fig. 10, where the dip near  $\varepsilon_{1,3}^{(0)} = \varepsilon_{2,1}^{(0)} = 43.36$  meV disappears.

The interference of the resonances is defined by two factors: (i) direct interference of two resonance states and (ii) interference through the background. The direct interference is the main effect for the chosen parameters of the antidots. It is easy to prove that KP states may be characterized by a parity so that  $V_{mm'}(x) = V_{mm'}(-x)$ . The matrix element in Eq. (37) for the quasibound states depends on the parities of the wave functions. For instance, there is a strong interference between the first (even) resonance of the second channel and the third (even) resonance of the first channel (Fig. 10). If the distance between the antidots is  $L=29.25$  nm, there is an overlap of the second (odd) resonance of the second channel and the third (even) resonance of the first channel for the energy  $\varepsilon_{2,2}^{(0)} = \varepsilon_{1,3}^{(0)} = 60.62$  meV. In this case, the resonances do not interact directly but there is weak interaction of the levels as a result of the interference through the background.

Notice that the formation of a miniband in the transmission resonances can be obtained if we consider a superlattice of antidots in the waveguide. For example, Joe *et al.*<sup>35</sup> have investigated the characteristics of transmission resonance in a quantum-dot superlattice, considering the aspect-ratio variation of two alternating potential heights in the quantum channel. In this system, well-arranged resonant peaks in the first miniband of each plateau are divided into paired peaks of two groups, which produce an extra gap inside each mini-



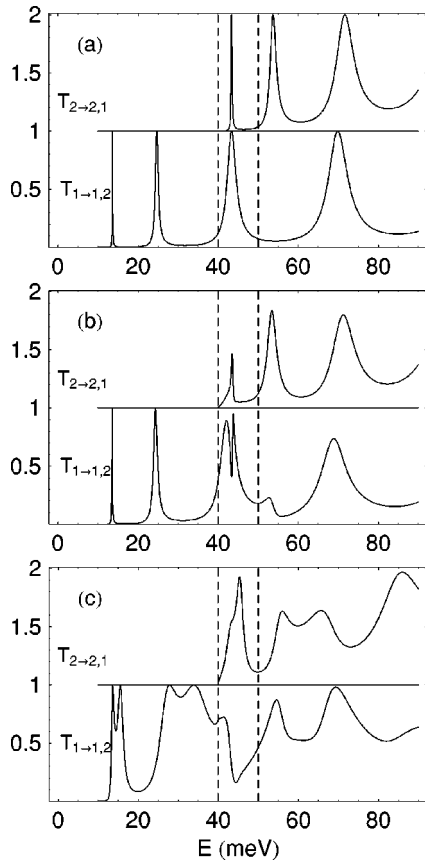


FIG. 9. Interference of two resonances in the transmission  $T_{1 \rightarrow 1,2}$  and  $T_{2 \rightarrow 2,1}$  for different positions of two antidots. The distance between the antidots is  $L=36.46$  nm, and the scattering parameter is  $aV_0=0.5$  eV nm. (a) There is a crossing of two BW resonances with the bare energy  $\epsilon_{1,3}^{(0)}=\epsilon_{2,1}^{(0)}=43.36$  meV for  $Y_c=0.5W$ . The overlapping of resonances in the first and the second channels produces a dip in the first channel of the transmission for both  $Y_c=(b) 0.4W$  and (c)  $0.3W$ .

band. As follows from our consideration, the phase structure of the resonances plays an important role in the formation of the band structure in open systems.

### B. Multiresonant interference in the continuum

A more general scenario of overlapping resonances is possible for three antidots in the waveguide. To understand the

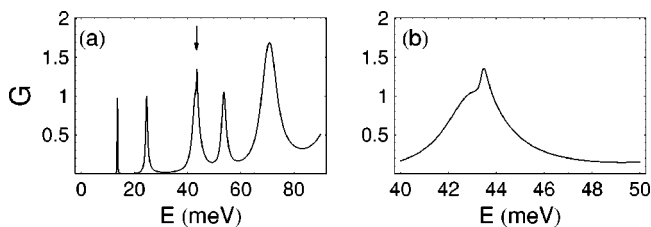


FIG. 10. (a) Conductance as a function of Fermi energy in the regime of the overlapping resonances (bare energies are  $\epsilon_{1,3}^{(0)}=\epsilon_{2,1}^{(0)}=43.36$  meV), presented in different channels. (b) Expanded plot of the conductance near the crossing of resonances is shown for  $Y_c=0.3W$ . Parameters of the system are the same as in Fig. 9.

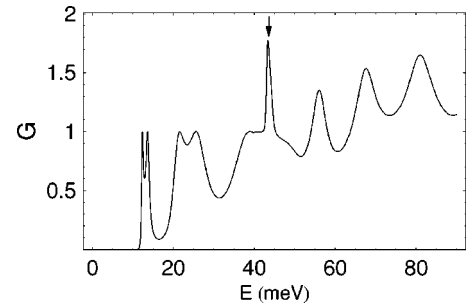


FIG. 11. Conductance of the waveguide with three antidots (distance between the dots is  $L=33.5$  nm, and amplitude of the intermediate antidot potential is chosen to be 1.25 times larger than the others;  $Y_c=0.25W$ ). Fano interference of two nearly degenerate resonances results in full suppression of pair resonances as a result of different parities of the quasi bound states. [Here, the position of the second resonance (odd peak) in the second channel is indicated by an arrow.]

main idea, we study the solutions of the KP equation for three antidots with a matrix potential given by Eq. (27). Again, we begin by considering the case where the coupling matrix element is equal to zero ( $Y_c=0.5W$ ), and we assume that the intermediate barrier is very high. In this case, there is a group of nearly degenerate states (set of coupled narrow resonances in each open channel). We may consider a crossing of two group resonances by changing the distance between the antidots. Using a perturbation, we can have a linear combination of four waves and find four complex energies. This solution may be easily investigated numerically.

In Fig. 11, we have displayed the conductance of the waveguide with three antidots (distance between dots is  $L=33.3$  nm; the amplitude of the intermediate antidot potential is chosen as 1.25 larger than the others). When there is a crossing of levels with the same parities, the Fano interference of two nearly degenerate resonances completely suppresses the pair resonances in the transmission. [The position of the second resonance (odd peak) in the second channel is indicated by an arrow in Fig. 11.] This is due to the different parities of the quasibound states, which indicates that the effective interaction of the resonances depends on the parity of the quasibound levels. The interference from the group of resonances also depends on the parities of the KP states.

### V. CONCLUSION

Interference effects have been investigated in a quantum waveguide with repulsive potentials (antidots). In a waveguide with two antidots, we have observed interesting phenomena: the interference between the quasibound states of one channel and background states of the second channel, and the interference of resonant group states of different channels. In this case, the zero of the Fano resonance is shifted to the complex plane and the coupling parameter becomes complex. We have used the KP theory for the calculation of quasibound states and have developed a perturbation theory for nearly degenerate levels in the continuum.

Degeneracy of two quasibound states takes place in a waveguide with three antidots, where the interference of degenerate states may be considered. The Fano interference of two nearly degenerate resonances fully suppresses pair resonances in the transmission. We have found that this could be explained by the parities of the quasibound states. Our results have shown that the zero of the Fano resonance, arising from the interference between groups of states (quasibound or resonant states) with the continuum, is generally placed in the complex plane. It was shown that the profile of the Fano line in the transmission depends on the phase difference between the paths. The Fano resonance in the transmission may disappear for some parameters of the system. The operation of resonances in transmission gives a method of controlling quantum interference in nanostructures. The application of Fano resonances has been discussed in many references,<sup>15,21,22</sup> and a tunable Fano interferometer consisting of a quantum dot via tunneling to a 1D channel has been realized in an experiment to observe the Fano resonance which coexists with an interaction in the form of the Coulomb blockade.<sup>36</sup>

#### ACKNOWLEDGMENT

This work is supported by the Indiana 21st Century Research and Technology Fund.

#### APPENDIX A: KAPURA-PEIERLS APPROACH FOR ONE-CHANNEL SYSTEMS

Among many different approaches for investigating resonant states,<sup>25,31,32</sup> we use Kapura's and Peierls' approach<sup>25</sup> which gives orthogonal functions of the quasibound states. (For comparison, a nonorthogonal basis is obtained by Sigert's approach.<sup>32</sup>) In order to find the KP basis, we solve an auxiliary equation (10) in the potential region ( $X_L < x < X_R$ ) with boundary conditions (the left and right sides of the antidots are used as the lines which pass through the points  $x=X_L$  and  $x=X_R$ )

$$\left( \frac{\partial}{\partial x} + ik_2 \right) \phi_j(x) \Big|_{x=X_L} = 0 \quad \left( \frac{\partial}{\partial x} - ik_2 \right) \phi_j(x) \Big|_{x=X_R} = 0, \quad (\text{A1})$$

where  $k_2 = \sqrt{2m(E-E_2)}/\hbar$  is the wave vector of electrons in the second band, and  $\varepsilon_j$  denotes the complex eigenvalues. Because the boundary conditions Eq. (A1) are complex and uniform, the solutions of Eq. (10) have an infinite set of complex functions  $\phi_j(x)$  ( $j=1,2,\dots$ ) with the orthogonality conditions

$$(\phi_j | \phi_{j'}) \equiv \int_{X_L}^{X_R} \phi_j(x) \phi_{j'}(x) dx = \delta_{jj'}. \quad (\text{A2})$$

The orthogonality condition of Eq. (A2) can be obtained from the following steps: (a) write two KP equations for  $\phi_j$  and  $\phi_{j'}$  from Eq. (10), (b) multiply each equation by an orthogonal function, either  $\phi_{j'}$  or  $\phi_j$ , (c) integrate both equations in the interval  $X_L < x < X_R$  taking into account Eq. (A1),

and (d) substitute from one equation to the other. Notice that Eq. (A2) is the direct product of two functions (not the product of the one with the complex conjugate of the other).<sup>25</sup> Using Eqs. (10) and (A1), it is easy to show that the eigenvalues may be written as

$$\varepsilon_j = \varepsilon_j^R - i\gamma_j^R, \quad (\text{A3})$$

where  $\varepsilon_j^R$  are the real energies of the resonances, and  $\gamma_j^R$  are the real (and positive) widths of the resonances which are defined as

$$\gamma_j^R = \frac{\hbar^2 k_2 [|\phi_j(X_L)|^2 + |\phi_j(X_R)|^2]}{2m \int_{X_L}^{X_R} |\phi_j(x)|^2 dx} \geq 0. \quad (\text{A4})$$

The wave function  $\psi_2^{(0)}(x)$  for the second decoupled channel is the solution of the equation

$$\left( -\frac{\hbar^2}{2m} \frac{\partial^2}{\partial x^2} + V_{22}(x) \right) \psi_2^{(0)}(x) = (E - E_2) \psi_2^{(0)}(x). \quad (\text{A5})$$

On the other hand, the wave function  $\psi_2^{(0)}(x)$  may be expanded in the interval  $X_L < x < X_R$  as

$$\psi_2^{(0)}(x) = \sum A_j^{(0)} \phi_j(x). \quad (\text{A6})$$

Multiplying Eq. (10) by  $\psi_2^{(0)}(x)$  and Eq. (A5) by  $\phi_j(x)$ , subtracting one from the other after the integration of each equation over the interval  $X_L < x < X_R$ , and using the orthogonality conditions [Eq. (A2)], the amplitude  $A_j^{(0)}$  can be written as

$$A_j^{(0)} = \frac{i\hbar^2 k_2}{m} \frac{\phi_j(X_L)}{E - \varepsilon_j^R + i\gamma_j^R}. \quad (\text{A7})$$

Therefore, the wave function in the potential region may be written as

$$\psi_2^{(0)}(x) = \frac{i\hbar^2 k_2}{m} \sum_j \frac{\phi_j(x) \phi_j(X_L)}{E - \varepsilon_j^R + i\gamma_j^R}. \quad (\text{A8})$$

The transmission amplitude  $\tau_2$ , defined by  $\tau_2 e^{ik_2 X_R} = \psi_2^{(0)}(X_R)$ , can be expressed as

$$\tau_2 = \frac{i\hbar^2 k_2 e^{-ik_2 X_R}}{m} \sum_j \frac{\phi_j(X_R) \phi_j(X_L)}{E - \varepsilon_j^R + i\gamma_j^R}. \quad (\text{A9})$$

Notice that this transmission amplitude has resonant terms with a Lorentzian line shape.

#### APPENDIX B: KAPURA-PEIERLS APPROACH FOR COUPLED SYSTEMS

In this appendix, we extend the KP approach for two coupled resonant systems [Eqs. (29)] with boundary conditions

$$\left( \frac{\partial}{\partial x} + ik_1 \right) \phi_{1j}(x) \Big|_{x=X_L} = 0, \quad \left( \frac{\partial}{\partial x} - ik_1 \right) \phi_{1j}(x) \Big|_{x=X_R} = 0, \quad (\text{B1})$$

$$\left(\frac{\partial}{\partial x} + ik_2\right)\phi_{2j}(x)\Big|_{x=X_L} = 0, \quad \left(\frac{\partial}{\partial x} - ik_2\right)\phi_{2j}(x)\Big|_{x=X_R} = 0. \quad (\text{B2})$$

The orthogonality conditions can now be chosen as

$$(\phi_{1j}|\phi_{1j'}) + (\phi_{1j}|\phi_{1j'}) = \delta_{jj'}. \quad (\text{B3})$$

The complex eigenenergies have been written in the form  $\varepsilon_j = E_j^R - i\Gamma_j^R$  (see Sec. IV), where the width of the resonances is defined by

$$\Gamma_j^R = \frac{\hbar^2[k_1|\phi_{1j}(X_L)|^2 + k_2|\phi_{2j}(X_R)|^2]}{2m\int_{X_L}^{X_R} [|\phi_{1j}(x)|^2 + |\phi_{2j}(x)|^2]dx}. \quad (\text{B4})$$

Now, we focus on the scattering matrix when the electron waves are in two open channels. As a result of the linearity of the Schrödinger equation, we can consider the scattering of the two channels independently. For instance, if the incoming wave is only in the first scattering channel, the boundary conditions for the electron wave functions may be written as

$$\left(\frac{\partial}{\partial x} + ik_1\right)\psi_1(x)\Big|_{x=X_L} = 2ik_1, \quad \left(\frac{\partial}{\partial x} - ik_1\right)\psi_1(x)\Big|_{x=X_R} = 0, \quad (\text{B5})$$

$$\left(\frac{\partial}{\partial x} + ik_2\right)\psi_2(x)\Big|_{x=X_L} = 0, \quad \left(\frac{\partial}{\partial x} - ik_2\right)\psi_2(x)\Big|_{x=X_R} = 0. \quad (\text{B6})$$

The wave functions in the inner potential region may be expanded as Eqs. (30). By doing the same procedure as explained in Appendix A, we can find the amplitudes  $A_j$

$$A_j = \frac{i\hbar^2 k_1}{m} \frac{\phi_{1j}(X_L)}{E - E_j^R + i\Gamma_j^R}. \quad (\text{B7})$$

Then the wave functions in the inner region can be written as

$$\begin{aligned} \psi_1(x) &= \frac{i\hbar^2 k_1}{m} \sum_j \frac{\phi_{1j}(X_L)\phi_{1j}(x)}{E - E_j^R + i\Gamma_j^R}, \\ \psi_2(x) &= \frac{i\hbar^2 k_1}{m} \sum_j \frac{\phi_{1j}(X_L)\phi_{2j}(x)}{E - E_j^R + i\Gamma_j^R}. \end{aligned} \quad (\text{B8})$$

Therefore, the transmission amplitudes  $t_{11}, t_{12}, t_{21}$ , and  $t_{22}$  can be obtained from the boundary conditions, where the expressions for transmission amplitudes  $t_{11}$  and  $t_{21}$  are given in Eq. (31) in Sec IV.

- <sup>1</sup>S. Datta, *Electronic Transport in Mesoscopic Systems* (Cambridge University Press, Cambridge, U.K., 1995).
- <sup>2</sup>*Nanotechnology*, edited by G. L. Timp (Springer-Verlag, New York, 1999).
- <sup>3</sup>U. Fano, *Phys. Rev.* **124**, 1866 (1961).
- <sup>4</sup>R. K. Adair, C. K. Bockelman, and R. E. Peterson, *Phys. Rev.* **76**, 308 (1949).
- <sup>5</sup>U. Fano and A. R. P. Rau, *Atomic Collisions and Spectra* (Academic Press, Orlando, FL, 1986).
- <sup>6</sup>F. Cerdeira, T. A. Fjeldly, and M. Cardona, *Phys. Rev. B* **8**, 4734 (1973).
- <sup>7</sup>J. Faist, F. Capasso, C. Sirtori, K. W. West, and L. N. Pfeiffer, *Nature (London)* **390**, 589 (1997).
- <sup>8</sup>E. Tekman and P. F. Bagwell, *Phys. Rev. B* **48**, 2553 (1993).
- <sup>9</sup>S. A. Gurvitz and Y. B. Levinson, *Phys. Rev. B* **47**, 10578 (1993).
- <sup>10</sup>J. U. Nöckel and A. D. Stone, *Phys. Rev. B* **50**, 17415 (1994).
- <sup>11</sup>Zhi-an Shao, W. Porod, and C. S. Lent, *Phys. Rev. B* **49**, 7453 (1994).
- <sup>12</sup>D. Goldhaber-Gordon, H. Shtrikman, D. Mahalu, D. Abusch-Magder, U. Meirav, and M. A. Kastner, *Nature (London)* **391**, 156 (1998).
- <sup>13</sup>D. Goldhaber-Gordon, J. Göres, M. A. Kastner, H. Shtrikman, D. Mahalu, and U. Meirav, *Phys. Rev. Lett.* **81**, 5225 (1998).
- <sup>14</sup>C. S. Kim, A. M. Satanin, Y. S. Joe, and R. M. Cosby, *Phys. Rev. B* **60**, 10962, (1999).
- <sup>15</sup>J. Göres, D. Goldhaber-Gordon, S. Heemeyer, M. A. Kastner, H.

- Shtrikman, D. Mahalu, and U. Meirav, *Phys. Rev. B* **62**, 2188 (2000).
- <sup>16</sup>Ph. Durand, I. Páidarova, and F. X. Gadea, *J. Phys. B* **34**, 1953 (2001).
- <sup>17</sup>C. S. Kim, O. N. Roznova, A. M. Satanin, and V. B. Shtenberg, *JETP* **94**, 992 (2002).
- <sup>18</sup>Ph. Durand and I. Páidarova, *J. Phys. B* **35**, 469 (2002).
- <sup>19</sup>K. Kobayashi, H. Aikawa, S. Katsumoto, and Y. Iye, *Phys. Rev. Lett.* **88**, 256806 (2002).
- <sup>20</sup>U. F. Keyser, S. Borck, R. J. Haug, M. Bichler, G. Abstreiter, and W. Wegscheider, *Semicond. Sci. Technol.* **17**, L22 (2002).
- <sup>21</sup>J. F. Song, Y. Ochiai, and J. P. Bird, *Appl. Phys. Lett.* **82**, 4561 (2003).
- <sup>22</sup>D. E. Nikonov, A. Imamoglu, and M. O. Scully, *Phys. Rev. B* **59**, 12212 (1999).
- <sup>23</sup>H. Feshbach, *Ann. Phys. (N.Y.)* **5**, 357 (1958).
- <sup>24</sup>M. Goldberg and K. Watson, *Collision Theory* (Wiley, New York, 1964).
- <sup>25</sup>P. Kapura and R. Peierls, *Proc. R. Soc. London, Ser. A* **1966**, 277 (1938).
- <sup>26</sup>K. A. Matveev, *Phys. Rev. B* **51**, 1743 (1995).
- <sup>27</sup>A. Furusaki and K. A. Matveev, *Phys. Rev. Lett.* **75**, 709 (1995).
- <sup>28</sup>G. Hackenbroich and H. A. Weidenmüller, *Phys. Rev. Lett.* **76**, 110 (1996).
- <sup>29</sup>R. Landauer, *Philos. Mag.* **21**, 863 (1970).
- <sup>30</sup>M. Buttiker, *Phys. Rev. B* **35**, 4123 (1987).
- <sup>31</sup>G. Breit and E. Wigner, *Phys. Rev.* **49**, 519 (1936).

<sup>32</sup>A. J. F. Sigert, Phys. Rev. **56**, 750 (1939).

<sup>33</sup>G. García-Calderón, R. Romo, and A. Rubio, Phys. Rev. B **47**, 9572 (1993).

<sup>34</sup>Zhi-an Shao and W. Porod, Phys. Rev. B **51**, 1931 (1995).

<sup>35</sup>Y. S. Joe, D. S. Ikeler, R. M. Cosby, A. M. Satanin, and C. S. Kim, J. Appl. Phys. **88**, 2704 (2000).

<sup>36</sup>A. C. Johnson, C. M. Marcus, M. P. Hanson, and A. C. Gossard, Phys. Rev. Lett. **93**, 106803 (2004).